Forensic Sciences Research, 2025, Vol. 10, Issue 1
https://doi.org/10.1093/fsr/owae009
Research Article

Sex determination based on features of the craniofacial bones in a sample of the central Chinese population using cone beam computed tomography

Wei Zhang[1,†], Shuang Wu[2,†], Shangxun Li[3], Haisheng Wang[3], Mohong Deng[4], Liang Ren[1], Liang Liu[1] and Hongmei Dong[1,*]

[1]Department of Forensic Medicine, Tongji Medical College, Huazhong University of Science and Technology, Wuhan, China
[2]Department of Pathophysiology, School of Basic Medical Sciences, Wuhan University, Wuhan, China
[3]Institute of Forensic Science and Technology, Department of Public Security of Hubei Province, Wuhan, China
[4]Department of Oral and Maxillofacial Surgery, Key Lab for Oral Biomedical Engineering of Ministry of Education, School and Hospital of Stomatology, Wuhan University, Wuhan, China

*Corresponding author. E-mail: hongmeidong1@hotmail.com

†Wei Zhang and Shuang Wu contributed equally to this manuscript.

Abstract

Accurate determination of sex from the skeletal remains of unidentified individuals is challenging in forensic practice. The bone standards for sex determination are population and generation specific. The present study investigated the potential utility of the craniofacial bones as an indicator of sex in a contemporary sample of the central Chinese population. A total of 171 adults (75 male, 96 female) of known age and sex underwent cone beam computed tomography (CBCT). A three-dimensional image from skull CBCT was reconstructed using specialized software (SimPlant Pro, version 11.04). Eleven linear measurements were selected to be measured, nine of which were sexually dimorphic. Discriminant function analysis (DFA) and logistic regression analysis (LRA) were used to develop mathematical models for sex determination. The equations of various variable combinations achieved classification rates of 83.6% in DFA and 84.8% in LRA, with cross-validation rates >80%. Results of the present study indicated that the accuracy of the craniofacial bones to determine sex could reach >80%, and bizygomatic breadth was the most sexually dimorphic variable among the craniofacial bones.

Key points

- Sexual dimorphism of 11 linear dimensions of the craniofacial bones of a central Chinese population were studied.
- The accuracy of the craniofacial bones in determining sex was as high as 84.8%.
- The craniofacial bones were useful for determining sex in a sample of the central Chinese population.

Keywords: forensic anthropology; craniofacial bones; sex determination; Chinese population

Introduction

Sex determination by analyzing the human skeleton is an essential component of forensic practice [1, 2]. In some cases of mass disasters or crime scenes, biological samples containing genetic information may be difficult to obtain from severely decomposed or destroyed bodies, in which case fragmented bones may be used for identifying individuals [3].

The pelvis is acknowledged to be the most sexually dimorphic bone [4, 5]. Although sex dimorphism of the long bones has been shown to be better than that of the skull in some studies [6], the skull remains generally acknowledged as the second best indicator of sex after the pelvis [7, 8]. In addition, the skull is usually better preserved than the common long bones, and skull analysis also offers the potential for facial reconstruction [9].

To date, sex determination based on skull features has been mainly performed by morphological and metric evaluation [10]. Morphological evaluation is performed by visual observations that rely on subjective assessment. The five cranial traits (nuchal crest, mastoid process, glabella, supraorbital margin, and mental eminence) described by Walker are the most commonly used morphological indicators for sex determination [11, 12]. In the metric evaluation, the mastoid process is often used due to its stability, with up to 95% accuracy in determining sex [13–16]. In addition to the mastoid process, maximum cranial length, nasal height, bizygomatic width, glabella, frontal profile, and superciliary arch have also been measured for sex determination, with high reliability and accuracy [13, 17–19]. Results of previous studies indicated that the mandible also had a high sex determination value,

Received: July 5, 2023. **Accepted:** January 26, 2024

with an accuracy of 84.2% [20, 21]. In general, morphological evaluation has the advantages of speed, convenience, and direct estimation, while the metric method is more objective and accurate.

With the development of computer technologies, digital radiography and computed tomography (CT) have been applied to measurements in forensic anthropology [9, 22–25]. In the present study, we applied cone beam CT (CBCT), a type of CT that has been exclusively used in the oral and maxillofacial regions, which can provide reliable and legible images [21, 26] by projecting in three dimensions. Advantages of CBCT also include the clarity of the scans, fewer motion artifacts, and reduced radiation dose(s) to subjects [26].

Bone growth and development are influenced by changes in functional demands, nutritional supply, and environmental conditions [27–30]. However, the bone database of a particular population is not necessarily suitable for others due to inter- and intra-population variability [31]; moreover, patterns of sexual dimorphism vary dramatically even within a limited geographical region and historical period [12, 32, 33]. Therefore, collecting contemporary skeletal data and improving methods to update osteometric standards are necessary.

In the present study, we aimed to investigate sexual dimorphism of the craniofacial bones using discriminant function analysis (DFA) and logistic regression analysis (LRA) to determine the combination(s) of variables that provide optimal discrimination between the sexes in a sample of the central Chinese population.

Materials and methods

Sample description

Data used in the present study were derived from individuals (age >18 years) undergoing CBCT examination in the Department of Oral Radiology, Stomatology School, Wuhan University (Wuhan, China). Individuals of non-Han Chinese origin, those with injuries, previous surgical procedures, and craniofacial and/or growth abnormalities were excluded. CBCT data from 171 subjects (75 male, mean (±SD) age 41.2 ± 14.6 years; 96 female, mean (±SD) age 40.6 ± 12.7 years) were used with the institutional approval to be usual in this study, and written informed consent was obtained. There was no statistical difference in mean age between the males and females ($P > 0.05$). The ethical review exemption for this study was granted by the Ethics Committee of Tongji Medical College, Huazhong University of Science and Technology.

Skeletal measurements

CBCT images were obtained using a CBCT scanner (NewTom VG, QR Srl, Verona, Italy) and saved in a Digital Imaging and Communications in Medicine (i.e. "DICOM") format. The scanning parameters were as follows: scanning area, 23 cm × 17 cm (including the region of the entire skull); tube voltage, 120 kV; tube current, 5 mA; scanning time, 3.0 s; and pixel spacing, 0.3 mm. The DICOM files were imported into a workstation (SimPlant version 11.04; Dentsply Sirona, York, PA, USA). The soft tissue and shadow were removed and the bone tissue was separated into independent structures for subsequent measurements using the split-reconstruction tool in the software.

In accordance with previous reports [34–37], 11 linear measurements were selected. These 11 linear measurements and their corresponding abbreviations and definitions are summarized in Table 1. The 11 linear measurements were identified using rotation and zoom tools in three-dimensional (3D) images. A schematic representation of the linear measurements was marked on the 3D model shown in Figure 1. All linear measurements were measured directly by drawing lines between the chosen points, while the software provided corresponding measurements. Results were accurate to the nearest 0.01 mm. All measurements were recorded twice by two trained observers, and the mean values were subjected to statistical analysis.

Statistical analysis

To evaluate data quality and repeatability, 30 images were randomly selected and measured by two trained observers to assess intra- and inter-observer agreement by calculating the relative technical error of measurement (rTEM) and coefficient of reliability (R) before formal data collection [38, 39]. Values <1 for R and <2% for rTEM were acceptable. The values of rTEM (0.513%–1.920%) and R (0.818–0.994) are summarized in Table 2. The R values for the 11 variables were regarded as "almost perfect reliability," with higher R values indicating greater measurement reliability [40].

In descriptive statistics, mean, standard deviation (SD), and standard error of the mean (SEM) were calculated for each variable in both sexes. The Shapiro–Wilk test was used to determine whether the variables were normally distributed and Levene's test was used to examine the homogeneity

Table 1. Description and abbreviation of 11 linear measurements of the craniofacial bones.

No.	Abb.	Linear measurements	Description
1	MFH	Morphological facial height	Direct distance between nasion and gnathion
2	NPH	Nasion-prosthion height	Direct distance between nasion and exoprothion
3	FMT	Upper facial breadth	Direct distance between the two frontomalare temporale
4	ZYB	Bizygomatic breadth	Direct distance between the two zygion
5	MSB	Bimastoidal breadth	Direct distance between the two mastoideale
6	EKB	Biorbital breadth	Direct distance between the two ektokonchion
7	OBB	Orbital breadth	Direct distance between maxillofrontale and ektokonchion and the average on both sides
8	OBH	Orbital height	The height between the upper and lower borders of the orbit and the average on both sides
9	NLH	Nasal height	Direct distance between nasion and nasospinale
10	GND	Glabella-nasospinale distance	Direct distance between glabella and nasospinale
11	NLB	Nasal breadth	The distance between the anterior edges of the nasal aperture at its widest extent

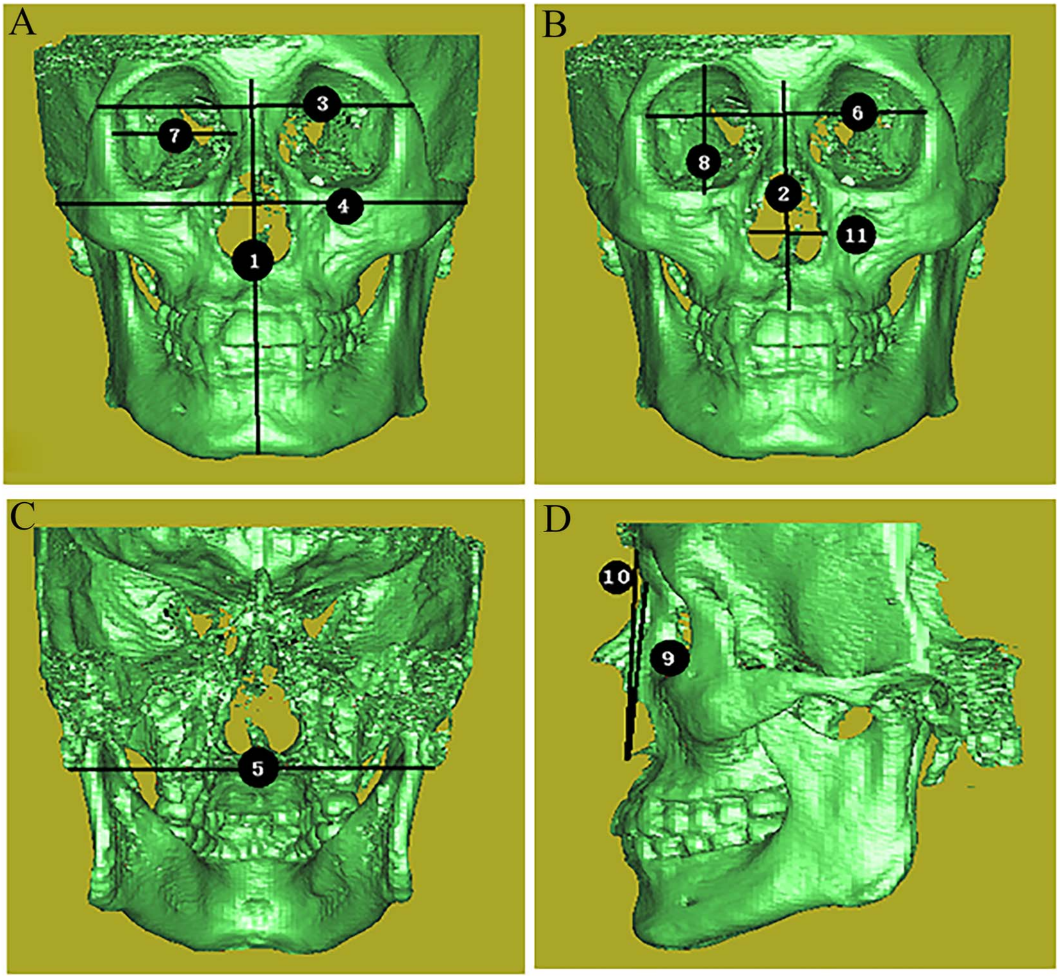

Figure 1 3D model of cranial-facial bones. Anterior view (A, B), posterior view (C), and left view (D). (1) Morphological facial height (MFH); (2) nasion-prosthion height (NPH); (3) upper facial breadth (FMT); (4) bizygomatic breadth (ZYB); (5) bimastoidal breadth (MSB); (6) biorbital breadth (EKB); (7) orbital breadth (OBB); (8) orbital height (OBH); (9) nasal height (NLH); (10) glabella-nasospinale distance (GND); (11) nasal breadth (NLB).

Table 2. Measurement precision of all the variables of the craniofacial bones.

No.	Variable	rTEM (%)	*R*
1	MFH	0.614	0.994
2	NPH	1.027	0.981
3	FMT	1.450	0.899
4	ZYB	0.513	0.991
5	MSB	1.425	0.873
6	EKB	0.874	0.963
7	OBB	1.064	0.818
8	OBH	1.322	0.828
9	NLH	1.759	0.917
10	GND	1.920	0.903
11	NLB	1.772	0.911

of variance. An independent *t*-test was used to assess the degree of significance between the two sexes. Variables with significant sex differences were further calculated using DFA and LRA to establish equations.

The data were first entered into univariate and direct multivariate DFA. In addition, a stepwise method was applied to select variables, included as $F > 3.84$ and rejected as $F < 2.71$, canonical discriminant function coefficients were extracted to form multivariate discriminant equations and the cut-off point was the mean value of the two group centroids. In application, higher values to the cut-off point were accepted to be male and lower values to be female, while equal values were classified as "indeterminate sex".

LRA was used to assess variables individually and in combination. Each independent variable's unique contribution was quantified to derive equations with different variable combinations and applied the Hosmer–Lemeshow to the goodness-of-fit test [41].

To quantify the effectiveness of the statistical models, the "leave-one-out" cross-validation method was used in DFA. The validation procedure added a cross-validated error rate at each step until the error rate could not be decreased. Receiver operating characteristic (ROC) curve, a well-accepted test measure of predictive accuracy [42], was used to assess the LRA models. Also, the exact cut-off values were calculated based on the trade-off between sensitivity and specificity from the corresponding Youden index. It was classified to be female when the measurement was greater than the exact cut-off value.

All statistical analyses were performed using Excel spreadsheet software (Microsoft Corporation, Redmond, WA, USA) and SPSS version 26.0 (IBM Corporation, Armonk, NY, USA). Differences with $P < 0.05$ were considered to be statistically significant.

Results

Descriptive analysis

The variables for two sexes were normally distributed with homogeneity of variance. Descriptions of the 11 variables are summarized in Table 3. The mean values for males were higher than those of females. The Student *t*-test identified nine variables, including morphological facial height (MFH), nasion-prosthion height (NPH), upper facial breadth (FMT), bizygomatic breadth (ZYB), bimastoidal breadth (MSB), biorbital breadth (EKB), orbital breadth (OBB), orbital height (OBH), and nasal height (NLH), which were statistically different between the two sexes ($P < 0.01$), with no differences in glabella-nasospinale distance (GND) and nasal breadth (NLB). The nine selected variables were entered into DFA and LRA.

Discriminant function analysis

Univariate DFA

Nine equations for the nine variables were tested by cross-validation and summarized in Table 4. ZYB was recognized to be the most sexually dimorphic, with a high classification accuracy rate (80.1%) (Equation Y1). The classification accuracy rates for MFH, FMT, and EKB were ~75%. The remaining five variables yielded lower correct prediction rates (<70%).

Multivariate DFA

The direct method achieved a greater level of classification accuracy than the stepwise method (Table 5). Equation Y2 employed all nine variables using the direct method and exhibited the best discriminatory values, with a correct classification for 84.0% of males and 83.3% of females. The stepwise method used four variables (MFH, NPH, ZYB, and OBB) by its default procedure to establish equation (Y3), attaining an accuracy rate of 82.5% with lower sex bias (0.4%). To handle cases with partial fragmentation of the craniofacial bones, an attempt was made to build equations Y4 to Y9 (Table 6) with highly relevant variables (ZYB > FMT > EKB = MFH) according to the correlation coefficient in the structure matrix, and achieved a sex classification accuracy >80%. For example, the incorporation of FMT and ZYB in the model (Y8) obtained a high correct classification rate of 82.5% with a sex bias of 7.5%.

Logistic regression analysis

Equations established by LRA are summarized in Tables 7–9. Only one univariable equation, ZYB, yielded an accuracy rate of 81.3% with sex bias of −7.1% (Y10). In the multivariate direct regression process, Y11 contained only eight variables because NLH was rejected for contributing little to the equation. Y11 achieved the highest accuracy rate (81.3% for males, 87.5% for females, 84.8% pooled). In the multivariate stepwise regression process, the forward conditional approach integrated four variables (MFH, NPH, ZYB, and EKB) into model Y12 and provided a correct classification of 81.9%. According to the variable contribution coefficients, some other combinations (Y13, Y14, Y15) were calculated, achieving comparatively good classification rates and model

Table 3. Descriptive statistics of the variables of the craniofacial bones.

No.	Variable	Male			Female			*P* value
		Mean ± SD	SEM	Range	Mean ± SD	SEM	Range	
1	MFH	121.58 ± 7.23	0.83	102.06–136.79	114.15 ± 8.33	0.85	67.83–130.80	<0.001*
2	NPH	73.14 ± 4.27	0.49	60.79–81.73	70.07 ± 4.53	0.46	60.52–81.91	<0.001*
3	FMT	108.51 ± 3.92	0.45	97.40–118.15	103.98 ± 5.57	0.57	66.04–115.83	<0.001*
4	ZYB	138.97 ± 4.86	0.56	121.29–147.63	131.55 ± 5.16	0.53	114.77–149.69	<0.001*
5	MSB	108.14 ± 4.45	0.51	96.95–117.07	104.25 ± 6.16	0.63	73.87–116.43	<0.001*
6	EKB	97.07 ± 3.70	0.43	87.32–108.35	93.31 ± 3.59	0.37	84.98–101.28	<0.001*
7	OBB	38.23 ± 2.77	0.32	33.80–44.25	36.34 ± 3.06	0.31	20.23–43.38	<0.001*
8	OBH	37.51 ± 2.00	0.23	33.65–43.14	36.28 ± 2.10	0.21	31.04–42.93	<0.001*
9	NLH	55.42 ± 3.01	0.35	48.65–63.00	52.72 ± 3.44	0.35	45.93–61.73	<0.001*
10	GND	65.86 ± 3.80	0.44	52.18–77.05	65.40 ± 3.91	0.40	57.07–75.64	0.440
11	NLB	25.92 ± 2.57	0.30	20.48–37.85	25.24 ± 2.13	0.22	19.76–35.69	0.065

*$P < 0.001$, independent *t*-test.

Table 4. Univariate discriminant function analysis of the craniofacial bones.

Function	Eigen value	Canonical correlation	Wilk's Lambda	Group centroids		Accuracy (%)			
				Male	Female	Original			Cross-validation
						Male	Female	Pooled	
$-16.693 + 0.142 \times$ MFH	0.271	0.426	0.787	0.586	−0.458	73.3	75.0	74.3	74.3
$-16.169 + 0.226 \times$ NPH	0.120	0.328	0.893	0.390	−0.305	68.0	64.6	66.1	66.1
$-25.664 + 0.241 \times$ FMT	0.326	0.496	0.754	0.643	−0.502	77.3	77.1	77.2	77.2
$-26.805 + 0.199 \times$ ZYB[a]	0.542	0.593	0.649	0.828	−0.647	82.7	78.1	80.1	80.1
$-21.106 + 0.198 \times$ MSB	0.164	0.375	0.859	0.455	−0.355	68.0	62.5	64.9	62.6
$-26.051 + 0.274 \times$ EKB	0.271	0.462	0.786	0.586	−0.458	74.7	69.8	71.9	74.9
$-13.719 + 0.367 \times$ OBB	0.168	0.379	0.856	0.461	−0.360	66.7	67.7	67.3	64.9
$-17.902 + 0.486 \times$ OBH	0.090	0.287	0.918	0.337	−0.263	56.0	59.4	57.9	57.9
$-16.255 + 0.301 \times$ NLH	0.171	0.381	0.855	0.464	−0.363	64.0	69.8	67.3	67.3

[a] $Y1 = -26.805 + 0.199 \times$ ZYB.

Table 5. Multivariate discriminant function analysis of the craniofacial bones.

Function	Coefficient		Eigen value	Canonical correlation	Wilk's Lambda	Group centroids		Accuracy (%)			
	Standardized	Unstandardized				Male	Female	Original			Cross-validation
								Male	Female	Pooled	
Direct											
MFH	0.664	0.094	0.737	0.651	0.576	0.965	−0.754	84.0	83.3	83.6	80.9
NPH	−0.558	−0.126									
FMT	0.224	0.054									
ZYB	0.576	0.115									
MSB	0.121	0.024									
EKB	0.108	0.030									
OBB	0.284	0.104									
OBH	0.097	0.047									
NLH	0.039	0.012									
Y2=−29.247+0.094×MFH−0.126×NPH+0.054×FMT+0.115×ZYB+0.024×MSB+0.030×EKB+0.104×OBB+0.047×OBH+0.012×NLH											
Stepwise											
MFH	0.701	0.100	0.708	0.644	0.586	0.946	−0.739	82.7	82.3	82.5	81.9
NPH	−0.493	−0.112									
ZYB	0.703	0.140									
OBB	0.316	0.116									
Y3=−26.907 + 0.100 × MFH − 0.112 × NPH + 0.140 × ZYB + 0.116 × OBB											

Table 6. Discriminant function analysis of the other highly relevant variables in the craniofacial bones.

Discriminant function (*P* > 0 is a male)	Accuracy (%)			
	Original			Cross-validation
	Male	Female	Pooled	
Y4 = −29.192 + 0.046 × MFH + 0.033 × FMT + 0.136 × ZYB + 0.020 × EKB	84.0	80.2	81.9	80.1
Y5 = −26.198 + 0.970 × MFH −0.094 × NPH + 0.159 × ZYB	81.3	81.3	81.3	80.1
Y6 = −28.929 + 0.049 × MFH + 0.143 × ZYB + 0.042 × EKB	84.0	79.2	81.3	79.5
Y7 = −29.027 + 0.055 × FMT + 0.159 × ZYB + 0.017 × EKB	88.0	78.1	82.5	81.3
Y8 = −28.745 + 0.065 × FMT + 0.162 × ZYB	86.7	79.2	82.5	81.9
Y9 = −28.567 + 0.174 × ZYB + 0.054 × EKB	84.0	77.1	80.1	80.1

Table 7. Univariate logistic regression analysis of the craniofacial bones.

Function	SE	Wald	Hosmer–Lemeshow	*P*	Exp(*B*)	Accuracy (%)			AUC area	Cut-off value
						Male	Female	Pooled		
17.558 – 0.147 × MFH	0.027	29.713	0.059	0.00	0.863	64.0	79.2	72.5	0.775	
11.484 – 0.157 × NPH	0.038	16.694	0.608	0.00	0.855	49.3	74.0	63.2	0.699	
30.039 – 0.279 × FMT	0.049	29.150	0.056	0.00	0.769	68.0	82.3	76.0	0.805	
40.783 – 0.299 × ZYB[a]	0.046	43.088	0.342	0.00	0.741	77.3	84.4	81.3	0.874	0.683
17.950 – 0.166 × MSB	0.037	20.585	0.986	0.00	0.750	52.0	76.0	65.5	0.714	
27.652 – 0.288 × EKB	0.053	30.483	0.185	0.00	0.744	64.0	79.2	72.5	0.769	
11.395 – 0.297 × OBB	0.064	21.448	0.625	0.00	0.743	46.7	74.0	62.0	0.713	
11.164 – 0.296 × OBH	0.083	12.819	0.139	0.00	0.744	42.7	78.1	62.6	0.650	
13.539 – 0.246 × NLH	0.053	21.867	0.733	0.00	0.782	58.7	75.0	67.8	0.731	

[a] **Y10** = 40.783 – 0.299 × ZYB.

fit indices, among which Y14 performed the best (81.3% for males, 85.4% for females, 83.6% pooled) with MFH and ZYB, with a sex bias of 4.1%.

Model diagnostic analysis

The cross-validation classification accuracy rate of the DFA models (Y1–Y9) was 79.5%–81.9%. The area under ROC curves (AUC) of the LRA models (Y10 to Y15) was accepted to be "reliable" (0.874–0.892).

Discussion

In our study, ZYB was recognized to be the most sexually dimorphic variable, either as single feature (Y1 and Y10) or in combination with other variables. The sexual dimorphism of ZYB was similarly reported in several previous studies, with accuracies of 78.3%–85.5% [43–45]. GND and NLB exhibited no difference among the Chinese Uygur [46], which were in accord with the contemporary central Chinese population of the present study. Furthermore, in studies of

Table 8. Multivariate logistic regression analysis of the craniofacial bones.

Function	*B*	SE	Wald	*P*	Exp(*B*)	Accuracy (%)			Hosmer–Lemeshow	AUC area	Cut-off value
						Male	Female	Pooled			
Direct											
MFH	−0.200	0.071	7.883	0.005	0.820	81.3	87.5	84.8	0.064	0.892	0.486
NPH	0.296	0.117	6.459	0.011	1.360						
FMT	−0.120	0.084	2.034	0.154	0.889						
ZYB	−0.203	0.064	9.989	0.002	0.819						
MSB	−0.048	0.049	0.984	0.321	0.953						
EKB	−0.100	0.099	1.016	0.313	1.100						
OBB	−0.178	0.094	3.571	0.059	0.842						
OBH	−0.100	0.124	0.644	0.422	0.903						
Y11 Logit $P = 48.940 - 0.200 \times MFH + 0.296 \times NPH - 0.120 \times FMT - 0.203 \times ZYB - 0.048 \times MSB - 0.100 \times EKB - 0.178 \times OBB - 0.100 \times OBH$											
Stepwise											
MFH	−0.195	0.067	8.422	0.004	0.823	77.3	85.4	81.9	0.220	0.887	0.571
NPH	0.259	0.109	5.619	0.018	1.296						
ZYB	−0.234	0.051	21.295	0.000	0.791						
EKB	−0.177	0.081	4.812	0.028	0.838						
Y12 Logit $P = 43.045 - 0.195 \times MFH + 0.259 \times NPH - 0.234 \times ZYB - 0.177 \times EKB$											

Table 9. Logistic regression analysis of the other highly relevant variables in the craniofacial bones.

Logistic regression function ($P > 0$ is a male)	Accuracy (%)			Hosmer–Lemeshow	AUC area	Cut-off value
	Male	Female	Pooled			
Y13 Logit $P = 41.232 - 0.178 \times MFH + 0.214 \times NPH - 0.261 \times ZYB$	78.7	85.4	82.5	0.077	0.882	0.514
Y14 Logit $P = 42.469 - 0.640 \times MFH - 0.256 \times ZYB$	81.3	85.4	83.6	0.276	0.880	0.497
Y15 Logit $P = 41.546 - 0.032 \times NPH - 0.288 \times ZYB$	77.3	83.3	80.7	0.307	0.875	0.671

Asian populations in Northwest India [44], Malaysia [47], Thailand [48, 49], and Japan [45], NLH, EKB, and FMT also exhibited sexual dimorphism, with accuracies of 77.8%–93%. Although the variables selected in the above studies were not exactly the same as ours, the sex determination accuracy rate of the craniofacial bones was, nevertheless, generally high. Thus, the present study demonstrated the utility of the sexual dimorphism of the craniofacial bones in enabling accurate sex determination in a central Chinese population.

However, the sexual dimorphism of some variables in our study was contrary to other studies [50, 51]. These different results may be due to population heterogeneity, which may be influenced by ancestry, nutritional supply, and living habits [52, 53]. Therefore, collecting data from different regions and populations is necessary for improving the database for forensic anthropology.

We analyzed the accuracy of craniofacial bone variables in determining sex using univariate and multivariate methods. An anthropological study revealed that the more variables contained, the higher the accuracy of the discriminant functions achieved [54]. In our study, Y2 and Y11 with nine or eight variables did achieve high classification rates in multivariate DFA and LRA, respectively. However, the models with fewer variables are more applicable in fragmented craniofacial bones in forensic practice. For example, Y3 to Y9 are effective because they contain fewer but valid variables. In addition, LRA models with too many independent variables may cause a mathematically unstable result and limited generalizability beyond the present sample [55]. For example, model Y11 yielded lower overall model fit (according to the Hosmer–Lemeshow value), while models Y14 and Y15, with combinations of MFH, NPH, and ZYB, demonstrated good explanatory power and external validity. Selecting variables is complex and relying on automated variable selection is insufficient, as it tends to exploit random chance factors in the sample [55]. We should also be guided by professional knowledge and previous investigations to ensure stable outcomes.

In the present study, we used two statistical methods—DFA and LRA—which were applied based on four assumptions: absence of outliers; independence of errors; linearity between logit of the outcome and predictor variables; the absence of multi-observation collinearity among predictors [54]. In addition, two more assumptions need to be satisfied for DFA: multivariate normality; homogeneity of variance–covariance matrices within groups. Thus, LRA is simpler and more flexible. LRA enables not only the prediction of sex but also the estimation of the probability of an individual being male or female [56]. In the present sample, both in univariate analysis and multivariate analysis, LRA equations (80.7%–84.8%) had slightly better classifying ability than DFA equations (80.1%–83.6% pooled). The present study demonstrated that LRA was a good alternative, although DFA was widely used for sex classification in previous studies.

Conclusion

Results of the present study demonstrated that the craniofacial bones of the central Chinese population were useful for classifying sex, and statistical models achieved accuracy rates >80%. We also derived equations that cover various conditions of highly relevant variables of the craniofacial bones, which can increase the scope of application to complex cases for sex determination.

Acknowledgements

We would like to thank Editage (www.editage.cn) for English language editing.

Authors' contributions

Wei Zhang and Shuang Wu collected and analyzed the data and drafted the manuscript; Shangxun Li and Haisheng Wang contributed to the design of the study; Deng Mohong collected the samples and contributed to the usage of the software; Liang Ren and Liang Liu participated in the discussions of the study; Hongmei Dong participated in the coordination of the study and revised the work critically for important intellectual content. All authors contributed to the final text and approved it.

Compliance with ethical standards

The ethical review exemption for this study was granted by the Ethics Committee of Tongji Medical College, Huazhong University of Science and Technology. The written informed consents were obtained.

Disclosure statement

No potential conflict of interest was reported by the authors.

Funding

This work was supported by the Ministry of Public Security of the People's Republic of China [Grant No. 2016JSYJB02]; Department of Forensic Medicine, Huazhong University of Science and Technology [under Grant No. 2017FYDC001].

References

1. Keen JA. A study of the differences between male and female skulls. Am J Phys Anthropol. 1950;8:65–80.
2. Hunt EE Jr, Gleiser I. The estimation of age and sex of preadolescent children from bones and teeth. Am J Phys Anthropol. 1955;13: 479–487.
3. Liebenberg L, Krüger GC, L'Abbé EN, et al. Postcraniometric sex and ancestry estimation in South Africa: a validation study. Int J Leg Med. 2019;133:289–296.
4. Bruzek J. A method for visual determination of sex, using the human hip bone. Am J Phys Anthropol. 2002;117:157–168.
5. Colman KL, van der Merwe AE, Stull KE, et al. The accuracy of 3D virtual bone models of the pelvis for morphological sex estimation. Int J Leg Med. 2019;133:1853–1860.
6. Spradley MK, Jantz RL. Sex estimation in forensic anthropology: skull versus postcranial elements. J Forensic Sci. 2011;56:289–296.
7. Nikita E, Michopoulou E. A quantitative approach for sex estimation based on cranial morphology. Am J Phys Anthropol. 2018;165:507–517.
8. Bertsatos A, Papageorgopoulou C, Valakos E, et al. Investigating the sex-related geometric variation of the human cranium. Int J Leg Med. 2018;132:1505–1514.
9. Sakuma A, Ishii M, Yamamoto S, et al. Application of postmortem 3D-CT facial reconstruction for personal identification. J Forensic Sci. 2010;55:1624–1629.
10. Yang W, Zhou M, Zhang P, et al. Skull sex estimation based on wavelet transform and Fourier transform. Biomed Res Int. 2020;2020:8608209.
11. Shim YT, Kim DI, Aum N, et al. Statistical classification methods for estimating sex based on five skull traits: a nonmetric assessment using 3D CT models. Homo. 2023;74:45–54.
12. Walker PL. Sexing skulls using discriminant function analysis of visually assessed traits. Am J Phys Anthropol. 2008;136:39–50.
13. da Silva JC, Strazzi-Sahyon HB, Nunes GP, et al. Cranial anatomical structures with high sexual dimorphism in metric and morphological evaluation: a systematic review. J Forensic Leg Med. 2023;99:102592.
14. Petaros A, Sholts SB, Čavka M, et al. Sexual dimorphism in mastoid process volumes measured from 3D models of dry crania from mediaeval Croatia. Homo. 2021;72:113–127.
15. Kemkes A, Göbel T. Metric assessment of the "mastoid triangle" for sex determination: a validation study. J Forensic Sci. 2006;51: 985–989.
16. de Paiva LA, Segre M. Sexing the human skull through the mastoid process. Rev Hosp Clin Fac Med Sao Paulo. 2003;58:15–20.
17. Meral O, Meydan R, Toklu BB, et al. Estimation of sex from computed tomography images of skull measurements in an adult Turkish population. Acta Radiol. 2022;63:1513–1521.
18. Čechová M, Dupej J, Brůžek J, et al. Sex estimation using external morphology of the frontal bone and frontal sinuses in a contemporary Czech population. Int J Leg Med. 2019;133:1285–1294.
19. Franklin D, Cardini A, Flavel A, et al. Estimation of sex from cranial measurements in a Western Australian population. Forensic Sci Int. 2013;229:158.e1–158.e8.
20. Dong H, Deng M, Wang W, et al. Sexual dimorphism of the mandible in a contemporary Chinese Han population. Forensic Sci Int. 2015;255:9–15.
21. Deng M, Bai R, Dong H, et al. Sexual determination of the mandible breadth in a central Chinese population sample: a three-dimensional analysis. Aust J Forensic Sci. 2016;49:332–343.
22. Stull KE, Tise ML, Ali Z, et al. Accuracy and reliability of measurements obtained from computed tomography 3D volume rendered images. Forensic Sci Int. 2014;238:133–140.
23. Oura P, Karppinen J, Niinimäki J, et al. Sex estimation from dimensions of the fourth lumbar vertebra in Northern Finns of 20, 30, and 46 years of age. Forensic Sci Int. 2018;290:350.e1–350.e6.
24. Ismail NA, Abdullah N, Mohamad Noor MH, et al. Accuracy and reliability of virtual femur measurement from CT scan. J Forensic Leg Med. 2019;63:11–17.
25. Krishan K, Chatterjee PM, Kanchan T, et al. A review of sex estimation techniques during examination of skeletal remains in forensic anthropology casework. Forensic Sci Int. 2016;261:165.e1–165.e8.
26. Hilgers ML, Scarfe WC, Scheetz JP, et al. Accuracy of linear temporomandibular joint measurements with cone beam computed tomography and digital cephalometric radiography. Am J Orthod Dentofacial Orthop. 2005;128:803–811.
27. Dunsworth HM. Expanding the evolutionary explanations for sex differences in the human skeleton. Evol Anthropol. 2020;29: 108–116.
28. Jantz RL, Meadows JL. Secular change in craniofacial morphology. Am J Hum Biol. 2000;12:327–338.
29. Kranioti EF, Işcan MY, Michalodimitrakis M. Craniometric analysis of the modern Cretan population. Forensic Sci Int. 2008;180:110.e1–110.e5.
30. Bruner E. Cranial shape and size variation in human evolution: structural and functional perspectives. Childs Nerv Syst. 2007;23: 1357–1365.
31. Plavcan JM. Sexual dimorphism in primate evolution. Am J Phys Anthropol. 2001;116:25–53.
32. Little BB, Buschang PH, Peña Reyes ME, et al. Craniofacial dimensions in children in rural Oaxaca, Southern Mexico: secular change, 1968–2000. Am J Phys Anthropol. 2006;131:127–136.
33. Oikonomopoulou EK, Valakos E, Nikita E. Population-specificity of sexual dimorphism in cranial and pelvic traits: evaluation of existing and proposal of new functions for sex assessment in a Greek assemblage. Int J Leg Med. 2017;131:1731–1738.

34. Jin D, Yu D, Pi Y. [Study on sex determination of the skull IV. Orbital and nasal parts]. J Med Sci Yanbian Univ. 1987;10: 246–249. Chinese.
35. Jin D, Yu D, Pi Y. [Study on sex determination of the skull III. Mastoid process]. J Med Sci Yanbian Univ. 1987;10:24–27. Chinese.
36. Caple J, Stephan CN. A standardized nomenclature for craniofacial and facial anthropometry. Int J Leg Med. 2016;130:863–879.
37. Xi H, Chen Z, editors. Anthropometric Methods. 2nd edition. Beijing (China): Science Press;2010. Chinese.
38. Langley NR, Meadows Jantz L, McNulty S, et al. Error quantification of osteometric data in forensic anthropology. Forensic Sci Int. 2018;287:183–189.
39. Goto R, Mascie-Taylor CG. Precision of measurement as a component of human variation. J Physiol Anthropol. 2007;26:253–256.
40. Bland JM, Altman DG. Statistical methods for assessing agreement between two methods of clinical measurement. Lancet. 1986;1: 307–310.
41. Blizzard L, Hosmer DW. Parameter estimation and goodness-of-fit in log binomial regression. Biom J. 2006;48:5–22.
42. Nick TG, Campbell KM. Logistic regression. Methods Mol Biol. 2007;404:273–301.
43. Zaafrane M, Ben Khelil M, Naccache I, et al. Sex determination of a Tunisian population by CT scan analysis of the skull. Int J Leg Med. 2018;132:853–862.
44. Kumar Battan S, Sharma M, Gakhar G, et al. Cranio-facial bones evaluation based on clinical CT data for sex determination in Northwest Indian population. Leg Med (Tokyo). 2023;64:102292.
45. Ogawa Y, Imaizumi K, Miyasaka S, et al. Discriminant functions for sex estimation of modern Japanese skulls. J Forensic Leg Med. 2013;20:234–238.
46. Yang W, Liu XN, Zhu F, et al. Sex recognition of skulls in Chinese Uygur. Fa Yi Xue Za Zhi. 2019;35:200–204. Chinese.
47. Syed Mohd Hamdan SN, Rahmat RA, Abdul Razak F, et al. Sex estimation of Malaysian sub-adults using craniometrics: a computed tomography study. Leg Med (Tokyo). 2023;64: 102275.
48. Mahakkanukrauh P, Sinthubua A, Prasitwattanaseree S, et al. Craniometric study for sex determination in a Thai population. Anat Cell Biol. 2015;48:275–283.
49. Beschiu LM, Ardelean LC, Tigmeanu CV, et al. Cranial and odontological methods for sex estimation—a scoping review. Medicina (Kaunas). 2022;58:1273.
50. Saini V, Srivastava R, Rai RK, et al. An osteometric study of Northern Indian populations for sexual dimorphism in craniofacial region. J Forensic Sci. 2011;56:700–705.
51. Gao H, Geng G, Yang W. Sex determination of 3D skull based on a novel unsupervised learning method. Comput Math Methods Med. 2018;2018:4567267–4567210.
52. Godde K. Secular trends in cranial morphological traits: a socioeconomic perspective of change and sexual dimorphism in North Americans 1849–1960. Ann Hum Biol. 2015;42:253–259.
53. Atkinson ML, Tallman SD. Nonmetric cranial trait variation and ancestry estimation in Asian and Asian-derived groups. J Forensic Sci. 2020;65:692–706.
54. Bartholdy BP, Sandoval E, Hoogland MLP, et al. Getting rid of dichotomous sex estimations: why logistic regression should be preferred over discriminant function analysis. J Forensic Sci. 2020;65:1685–1691.
55. Stoltzfus JC. Logistic regression: a brief primer. Acad Emerg Med. 2011;18:1099–1104.
56. Nikita E, Nikitas P. Sex estimation: a comparison of techniques based on binary logistic, probit and cumulative probit regression, linear and quadratic discriminant analysis, neural networks, and naïve Bayes classification using ordinal variables. Int J Leg Med. 2020;134:1213–1225.

Forensic Sciences Research, 2025, Vol. 10, Issue 1
https://doi.org/10.1093/fsr/owae009
Research Article